# Effect of Nonconjugated Polymers on the Conjugation Length and Structure of Poly(3-octylthiophene) in Ternary Polymer Blend

**Ying-Jie Huang,[1] Tar-Hwa Hsieh,[2] Yen-Zen Wang,[3] Ching-Nan Chuang,[2] Ya-Ping Chen,[2] Ping-Tsung Huang,[4] Ko-Shan Ho[2]**

[1]*Department of Biomedical Sciences, Chung Shan Medical University, Taichung 402, Taiwan*
[2]*Department of Chemical and Material Engineering, National Kaohsiung University of Applied Sciences, Kaohsiung 807, Taiwan*
[3]*Department of Chemical Engineering, National Yun-Lin University of Science and Technology, 640, Yun-Lin, Taiwan*
[4]*RITdisplay Corporation 12, Hsin Trsu Industrial Park, Hsin Tsu Sheng, Taiwan*

Received 26 January 2006; accepted 25 August 2006
DOI 10.1002/app.25616
Published online in Wiley InterScience (www.interscience.wiley.com).

**ABSTRACT:** The shifting of $\lambda_{max}$ ($\pi$-$\pi^*$ transition) of P3OT (poly(3-*n*-octylthiophene)) was used to monitor the degree of miscibility between P3OT and the matrix polymers. In the ternary blend system, 1% of P3OT is soluble in a uniform PMMA/EVA20 mixed matrix and does not interfere with the miscibility between PMMA and EVA20 (ethylene-vinyl acetate copolymer with 20% of vinyl acetate). But 5% of P3OT can attract EVA20 out of the matrix and induce the separation from 95% of PMMA/EVA20 matrix and cause the doublet peak of $\lambda_{max}$. Likewise, the DSC thermograms do not demonstrate the melting-point depression of EVA20 in a 5% P3OT ternary system. However, the melting-point depression did occur only for 1% of P3OT. IR-spectra demonstrate that the methylene groups affinity contributed to the misciblity either in 1% P3OT/PMMA or in P3OT (1 and 5%)/EVA20. The solubility difference of P3OT in PMMA (poor) and EVA20 (better) creates a continuous morphology for obtaining a highly conjugated path in a nonconjugated matrix. © 2007 Wiley Periodicals, Inc. J Appl Polym Sci 104: 773–781, 2007

**Key words:** phase separation; morphology; conjugated polymers

## INTRODUCTION

The behavior of rigid rod-flexible coil polymer mixtures has attained remarkable interest in both academic and industrial research. The achievement of molecularly dispersed rigid rods would result in molecular composites of high strength and toughness. As Flory[1] predicted with the lattice model for nematic state, the ordering of the rigid rods would reject the coil molecules. This incompatibility has been obtained in several investigations.[2] A high axial ratio of the rigid rod contributes to the demixing tendency according to the predictions.

The crystalline regions of poly(3-alkyl thiophene)s was characterized as the crystalline of the layered structure.[3–7] Since the discovery of this processing possibility of polyalkylthiophene (P3AT), several studies have involved mixing P3AT with various polymers or matrix offer commercial applications.[8–18] A common feature in most of the studies is the 16% percolation threshold for conjugation. This threshold agrees with the one calculated by the continuum percolation model for spherical particles.[19] Heeger et al.[20,21] have applied the shape of a rod-like particle with a decrease in dimensionality in the calculations for the percolation threshold and showed that the threshold can be obtained at low concentrations.

Rabeony et al.[22] reported, that the glass transitions were interactable in polythiophene/polystyrene blend, but this may be due to the applied pressure during the sample preparation. Homogenization by pressure has been previously applied for phase separation studies by Hashimoto.[23] Interestingly, in the above-mentioned studies, the threshold for percolation was found to be low (5–7%). Machado et al.[24] found percolation between 4 and 10% of the conjugated phase in poly(*p*-phenylenevinylene)/poly(ethylene oxide) blend, which was characterized as an immiscible blend. Laakso et al. found low degree of conjugation with 2–4% of P3OT in P3OT/EVA (ethylene-vinyl acetate copolymer) binary blending.[25] On the basis of these previous results, it is indicative that the degree of mixing may have an influence on the conditions for the $\pi$-electron conjugation.

P3OT was found to form a homogeneous phase in EVA20 (EVA with 20% vinylacetate) matrix up to 50% by optical microscopy (OM)[3] since P3OT can be easily

*Correspondence to:* K.-S. Ho (hks@cc.kuas.edu.tw).

Journal of Applied Polymer Science, Vol. 104, 773–781 (2007)

seen in the blended matrix under the OM because of its color. In the binary blend system containing more than 50% P3OT (P3OT in excess),[26] it is possible to form a continuous structure of P3OT-rich phase distributed within EVA20 matrix, which is one of the ideal topologies to create a high *p*-electron conjugation with lower percolation concentration.

When 80% P3OT was mixed with 20% EVA20,[26,27] it can form a well-defined continuous morphology, which can even be identified by naked eyes. However, the amount of P3OT in the blend system should be kept below 80% to obtain high conjugation. To reduce the concentration of the P3OT in the blend without loss of *p*-electron conjugation, a third phase that is not compatible with P3OT can behave as a matrix for the continuous structure. Consequently, a ternary blend of P3OT/PMMA/EVA20 was made by chloroform-casting on the glass plate in our laboratory to create a continuous structure of P3OT inside the larger continuous structure of PMMA/EVA20.

This study will focus on the addition of the third polymer in the binary P3OT/EVA20 blend to create a continuous P3OT-rich phase in the matrix with the least P3OT composition.

## EXPERIMENTAL

### Polymerization[7]

1-Bromoctane was reacted with magnesium to make a Grinard reagent followed by coupling with 3-bromothiophene, the monomer (3-octylthiophene) was then obtained and polymerized (oxidized by ferric chloride) in chloroform at 5–10°C in 1 h and precipitated into methanol followed by filtration. The obtained poly(3-octylthiophenes) (P3OT) were purified by dissolved in THF followed by precipitation in a methanol pool. After filtration, the wet P3OT cake was dried in a vacuum oven at 40°C for 16 h.

### Blending

PMMA (MW ~ 70,000) and EVA20 (MW ~ 80,000 with 20 mol % of vinyl acetate copolymerized with 80 mol % of ethylene) obtained from Polyscience Inc. were mixed individually with chloroform in 1% followed by stirring over nightly. To assure the entire dissolution of P3OT in chloroform, the concentration was reduced to 0.1%. The solid ratios in the blend were controlled by the mixing volumes of each neat polymer solution together (1% PMMA and EVA20 in chloroform, 0.1% P3OT in chloroform) followed by stirring over night. The polymer blend solution was then cast on a petri dish under a ventilated hood to remove chloroform solvent. The cast film was further dried in a vacuum oven at room temperature for more than 24 h.

**TABLE I**
**Assignments of the Solid-State $^{13}C$ CP/MAS NMR Spectrum of P3OT**

| Frequency (ppm) | Position of carbon |
|---|---|
| 136.5 | 4 |
| 133.0 | 1 |
| 131.0 | 3 |
| 126.0 | 2 |
| 33.2 | 5–6 (crystalline methylenes)[28,29] |
| 31.2 | 5–6 (amorphous methylenes)[28,29] |
| 24 | 11 |
| 15 | 8($-CH_3$) |

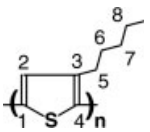


### Characterization

#### $^{13}$CCP/MAS NMR

Solid-state $^{13}C$ CP/MAS NMR experiments were performed for neat P3OT on a Bruker AVANCE-400 spectrometer, equipped with a Bruker double- tuned 7 mm probe, with resonance frequencies of 100.6 MHz for $^{13}C$ nuclei. The assignments of the characteristic $^{13}C$ CP/MAS NMR spectrum of neat P3OT are listed in Table I.

#### UV–vis

The UV–vis spectra of the samples were obtained from a Hitachi U-2000 at 50 nm/min. The wavelength ranged from 190 to 1100 nm and only the visible range is demonstrated (400–800 nm). The blending solution with various compositions are prepared by dipping the glass plates in polyblend solution, followed by being dried in a vacuum oven at room temperature for over 24 h.

#### Differential scanning calorimetry (DSC)

The melting point ($T_m$) and glass transitional point ($T_g$) of neat and blend samples were measured by a Perkin–Elmer DSC-7 at 10°C/min from 0°C to 200°C. Each sample weight was the same of about 10 mg.

#### Optical microscopy

The samples were obtained from evaporatively casting onto a microscope glass plate (7.6 × 2.54 × 0.1 $cm^3$) and kept at room temperature in open air for more than 24 h. An Olympus optical microscope (Mode BH-2) was used to take pictures of blend samples with 200 magnifications.

**TABLE II**
**Assignments of the P3OT IR-Spectrum**

| Frequency ($cm^{-1}$) | Assignment |
|---|---|
| 3050 | ν(—C=C—H) |
| 2955 | ν(—$CH_3$) |
| 2928 | ν(—$CH_2$—) |
| 2850 | ν(—CH—) |
| 1464 | δ(—$CH_3$) |
| 1376 | δ(—$CH_2$) |
| 823 | δ(C—S—C) |
| 720 | γ(—$CH_2$) |
| 670–599 | δ(C—S) |

FTIR

A Bio-Rad FTS-165 IR spectrometer was used to characterize neat P3OT and its blended samples which were mixed with KBr powders ground and pressed into tablets. The ranges of scanning were from 4400 to 400 $cm^{-1}$. The assignments of the characteristic IR absorption peaks of neat P3OT are listed in Table II.

## RESULTS AND DISCUSSION

### Characterization by solid state $C^{13}$ CP/MAS NMR

'The major absorption frequencies of solid state $C^{13}$ CP/MAS NMR of neat P3OT are assigned and listed in Table I. Each carbon is numbered according to the schematic diagram of P3OT chemical structure shown below Table I. The aliphatic side-chain carbons peak positions of *n*-octyl group of P3OT are around 15–40 ppm. The methyl group (—$CH_3$) contributes to the 15 ppm absorption and next to it is the methylene carbon, which gives an absorption peak at 24 ppm. The rest methylenes (numbered 5–10) show split peaks at 31.2 ppm from amorphous (gauche-) region and 33.2 ppm from crystalline (trans-) region.[28–29] The rest carbons of thiophene ring contribute to the peaks of 126 (numbered 2), 131 (numbered 3), 133 (numbered 1), and 136.5 (numbered 4), respectively.

### UV–vis spectra

A maximum absorbing wavelength ($\lambda_{max}$) within visible range contributes to the colors of the P3OT based blend systems and is designated as the π-π* transition of the P3OT backbones.[30] The location of the $\lambda_{max}$ depends on the length of the conjugation, longer conjugational length resulting in lower π-π* energy gap ($E_g = h\nu = hc/\lambda_{max}$) and higher $\lambda_{max}$. The conjugational length of P3OT can be altered by the interaction with matrix polymers resulting in a shifting of $\lambda_{max}$ (change of the conjugation length), the so-called solvatochromic effect. In other words, one can perceive the degree of miscibility of a conjugated polymer with other nonconjugated polymers merely from the shifting of its $\lambda_{max}$ or not. It will be confirmed and compared with by the regular characterization methods about the compatibility of polymer blends such as variation of glassy transitional temperature or melting-point depression, etc. Commonly, the presence of miscibility always contributes to a blue shift of $\lambda_{max}$ because of the interruption on the conjugation (flipping of the thiophene rings out of conjugated plane resulting in the reduction of coplanarity). P3OT that has a polar backbone (thiophene ring) and nonpolar side chain (octyl group) is proved to be soluble in polar (chloroform, THF, etc.) or nonpolar (toluene, hexane, decalin, etc.) solvents provides a more flexible choice of matrix polymers that are either polar or nonpolar.

The purpose for P3OT to obtain a continuous conjugated length with the least percentage in the nonconjugated matrix polymers can be more easily achieved by the polymer blend based on a ternary system when two kinds of polymers having distinguishingly different miscibilities with P3OT are chosen as the mixed matrix polymers. We shall check the critical miscible composition, which is defined as the composition when the $\lambda_{max}$ of P3OT stops shifting in each binary system (P3OT/PMMA and P3OT/EVA20). With the known critical composition obtained from individual binary system, the morphology and miscibility of the ternary system can be understood and controllable by altering the relative ratio between two matrix polymers.

The binary system of P3OT/EVA20 that has been proved to be compatible to each other by other methods[3,26] demonstrate a blue shift of $\lambda_{max}$ from 600 to 420 nm when mixed with EVA20 (Fig. 1) up to 50% of P3OT. Because of its excellent miscibility with P3OT, EVA20 can effectively disrupt the conju-

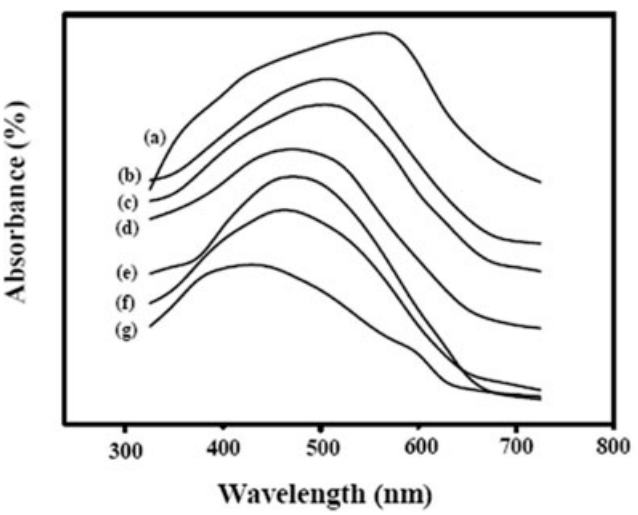


**Figure 1** UV–vis spectra of P3OT/EVA20 (a) neat P3OT, (b) 50/50, (c) 30/70, (d) 10/90, (e) 5/95, (f) 3/97, (g) 1/99.

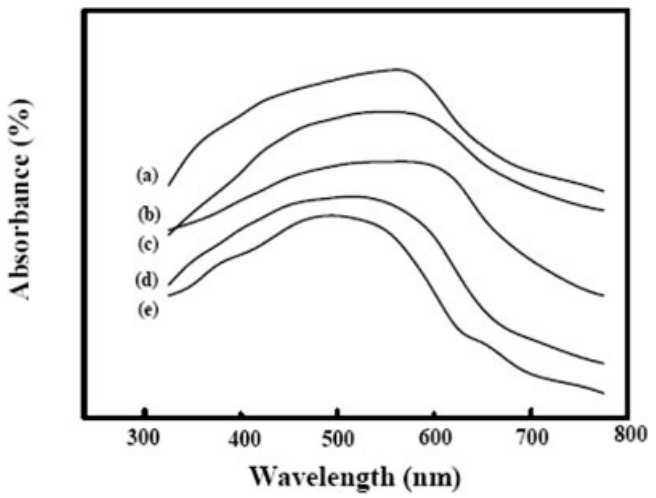


**Figure 2** UV–vis spectra of P3OT/PMMA (a) neat P3OT, (b) 50/50, (c) 5/95, (d) 2/98, (e) 1/99.

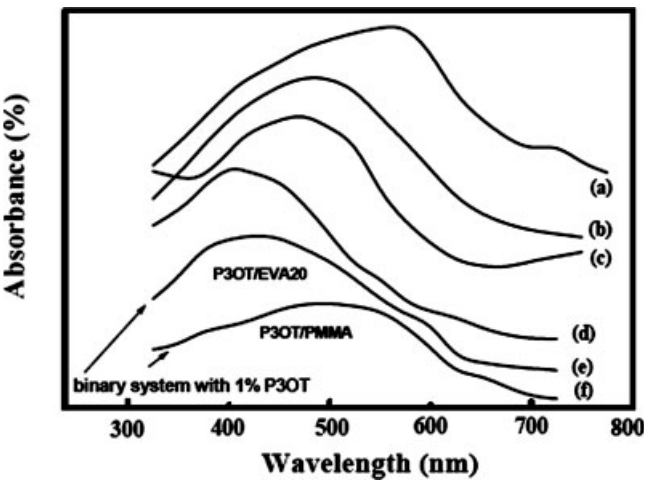


**Figure 3** UV–vis spectra of 1% of P3OT in ternary (P3OT/PMMA/EVA20) and binary systems: (a) neat P3OT, (b) 1/90/9, (c) 1/49.5/49.5, (d) 1/9/90, (e) P3OT/EVA20 1/99, (f) P3OT/PMMA 1/99.

gation length and changes the color of P3OT from red to yellow or even blue. As will be seen that the miscibility between P3OT and EVA20 can induce a melting-point depression of EVA20 in the blends from the thermal analysis of DSC measurement.

However, the $\lambda_{max}$ of P3OT/PMMA as shown in Figure 2 demonstrates the blue shift only when P3OT composition is below 5%. Above 5%, the P3OT is not soluble in PMMA matrix and the $\lambda_{max}$ remains at the same position with that of neat P3OT, which means no further conjugational interruption is induced by PMMA any more.

Favorable miscibility of P3OT with EVA20 than with PMMA comes from the bountiful ethylene groups of EVA20, which can interrupt the conformation of methylene side chains of P3OT from trans to gauche mode[3,27] and subsequently induces the flipping of main chain thiophene rings, resulting in the losing of coplanarity and conjugation.

The ternary system of P3OT/PMMA/EVA20 with 1% P3OT demonstrates a similar result with binary system of P3OT/EVA20 and P3OT/PMMA, respectively. Blue shift gradually disappears when PMMA is increased as shown from Figure 3(b–d) where $\lambda_{max}$ shift back close to that of neat P3OT from 475 to 530 nm. On the contrary, the blue shift enhances [Fig. 3(b–d)] when the relative ratio of EVA20 is increased in the ternary system. Likewise, when 5% of P3OT is present in the ternary blend, the blue shift of $\lambda_{max}$ is also found when EVA20 dominates as shown in Figure 4(e) but additional $\lambda_{max}$ peak with higher wavelength close to that of neat P3OT is found for higher PMMA percentages according to Figure 4(c,d). The extra absorption peak represents the presence of the immiscible domain at PMMA dominating compositions. As even higher composition of PMMA, the absorption peak with the lower wavelength disappears from Figure 4(b) because of the total immiscible occurrence in the ternary system.

### Differential scanning calorimeter

Two kinds of primary transitions of $T_{m1}$ (low) and $T_{m2}$ (high) are found in the thermograms of neat EVA20, in which the first melting at $T_{m1}$ is accompanied by the recrystallization and the formation of the crystalline phase with higher $T_{m2}$. When ratio of PMMA/EVA20 are varied in 1% P3OT ternary blend, $T_{m1}$ are depressed with the increasing PMMA and $T_{m2}$ remains at the same position (Fig. 5 and Table III). It indicates PMMA is miscible with EVA20 and 1% P3OT is uniformly distributed in the misci-

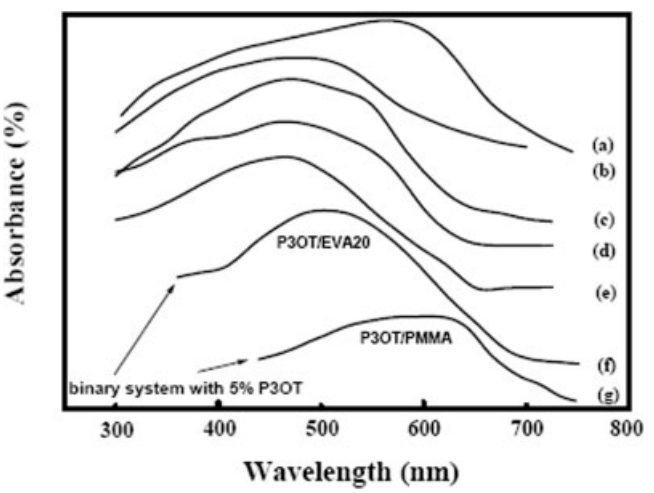


**Figure 4** UV–vis spectra of 5% of P3OT in ternary (P3OT/PMMA/EVA20) and binary systems: (a) neat P3OT, (b) 5/90/5, (c) 5/55/40, (d) 5/47.5/47.5, (e) 5/5/90, (f) P3OT/EVA20 5/95, (g) P3OT/PMMA 5/95.

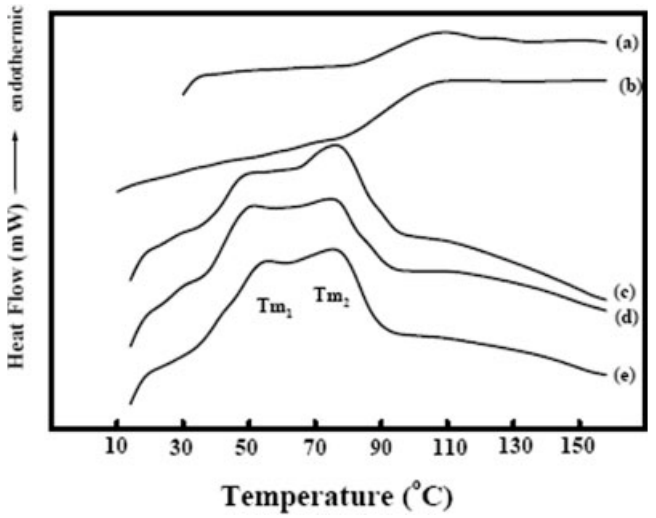


**Figure 5** DSC thermograms of 1% P3OT/PMMA/EVA20 system (a) neat PMMA, (b) 1/90/9, (c) 1/49.5/49.5, (d) 1/9/90, (e) neat EVA20.

ble PMMA/EVA20 matrix[31–34] of different PMMA and EVA20 ratios. This phenomenon has been confirmed in the discussion of UV–vis spectra based on Figure 3(b–d). From Figure 5, we can see the both $T_{m1}$ and $T_{m2}$ of EVA20 disappear when the composition of PMMA is increased to 90%, which means EVA20 is not able to crystallize and is well distributed in the PMMA dominated matrix. The presence of the $T_g$ depression of PMMA in the ternary blend when compared with that of neat PMMA (Fig. 5 and Table III) indicates that the miscibility between EVA20 and PMMA is still present and contributes to the $T_{m1}$ depression.

When P3OT is increased to 5% in the ternary system, both the $T_{m1}$ and $T_{m1}$ depression of EVA20 are not significant even for the high percentages of EVA20 according to Figure 6(c,d) and Table III because of the strong interactions between EVA20 and P3OT in the ternary blend. However, the $T_g$ of PMMA remains the same for 47.5% PMMA in the ternary system as shown in Figure 6(c), illustrating most of PMMA is phase-separated from the ternary blend. On that condition, the ternary blend is roughly divided into two kinds of domains including also pure PMMA domain and a uniformly mixed domain of P3OT and EVA20 almost excluding PMMA. Since most of the P3OT remains in the mixed domain of P3OT/EVA20 and PMMA is excluded outside, the composition of P3OT in the mixed domain is more than 5% (if PMMA is totally excluded, the compositions of P3OT are about $5/(5 + 90) = 5.26\%$ for 5/5/90 and $5/(5 + 47.5) = 9.5\%$ for 5/47.5/47.5, respectively,), resulting in a poorer miscibility of P3OT in EVA20 and red-shifts the $\lambda_{max}$ referring to Figure 1. Briefly, 5% of P3OT does induce a phase separation of PMMA out from the ternary system,

**TABLE III**
**$T_m$ (°C) and $T_g$ (°C) of P3OT/PMMA/EVA20 System**

| | 1% P3OT | 5% P3OT |
|---|---|---|
| Pure PMMA ($T_g$) | $T_g = 101$ | $T_g = 101$ |
| 1/90/9 | $T_g = 100$ | – |
| 1/49.5/49.5 | $T_{m1} = 48$, $T_{m2} = 75$ | – |
| 1/9/90 | $T_{m1} = 49$, $T_{m2} = 75$ | – |
| 5/5/90 | – | $T_g = 101$ |
| 5/47.5/47.5 | – | $T_{m1} = 51$, $T_{m2} = 75$, $T_g = 101$ |
| 5/5/90 | – | $T_{m1} = 51$, $T_{m2} = 76$ |
| Pure EVA20 ($T_m$) | $T_{m1} = 51$, $T_{m2} = 75$ | $T_{m1} = 51$, $T_{m2} = 75$ |

which allows us to control the morphologies of the ternary blend as will be discussed with the optical pictures.

## Optical microscopy

Ternary system with small percentages of P3OT is prepared to create a continuous conjugated strip in the matrix. In 1% P3OT system, three different compositions were prepared including 1/90/9 in which PMMA is dominant and 1/49.5/49.5 with equal amount of PMMA and EVA20, and 1/9/90 with EVA20 in excess.

When the composition of EVA20, as shown in Figure 7(a), is increased to 90% (1/9/90), the sample color is light but the film is sticky and cannot be easily separated from the glass plate. In 1% ternary system, the relative composition of P3OT in EVA20 without considering PMMA is equal to 1.11% and P3OT is uniformly distributed even though the relative composition of P3OT to PMMA now is increased to 10% (1/9), without considering EVA20, which is over the critical solubility of P3OT in PMMA. Therefore,

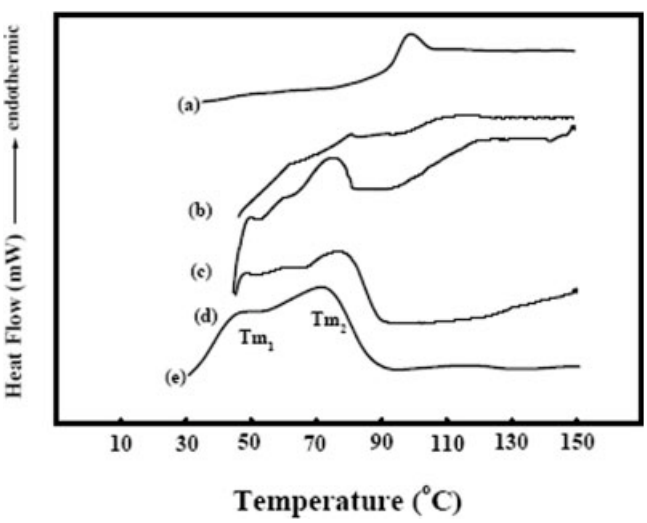


**Figure 6** DSC thermograms of 5% P3OT/PMMA/EVA20 system (a) neat PMMA, (b) 5/90/5, (c) 5/47.5/47.5, (d) 5/5/90, (e) neat EVA20.

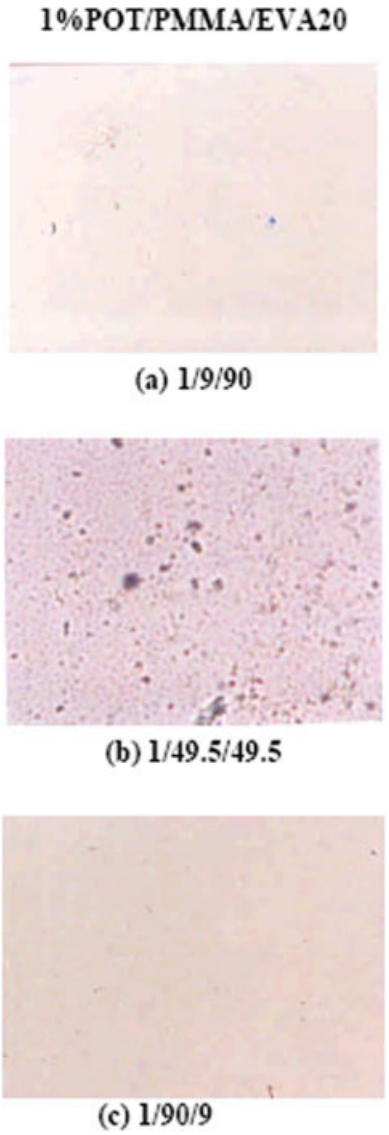


**Figure 7** Optical pictures of 1% P3OT/PMMA/EVA20 with ×100 (a) 1/9/90, (b) 1/49.5/49.5, (c) 1/90/9. [Color figure can be viewed in the online issue, which is available at www.interscience.wiley.com.]

the favorable interaction between the P3OT and EVA20 might prevent the precipitation of P3OT molecules out from PMMA/EVA20 matrix.

When PMMA and EVA20 were mixed in a equal composition [1/49.5/49.5; Fig. 7(b)] in the ternary blend, the cast film still looks uniform, which illustrates 1% P3OT is still soluble in the matrix with equal composition of PMMA and EVA20. If one of the matrix polymers (PMMA or EVA20) is neglected, the relative composition of P3OT in PMMA or EVA20 is about 2%, respectively, and P3OT is still soluble in either matrix with this small percentage according to Figures 1 and 2.

In PMMA-rich system (1/90/9), the cast-film, as shown in Figure 7(c), demonstrates a light color and sample is fragile because of the dominated glassy PMMA. The film looks homogeneous under the OM resulting from 1% P3OT is highly soluble in PMMA/EVA20 matrix. Besides, PMMA is possibly miscible with EVA20 in that ratio (PMMA/EVA20 = 90/9). Therefore, 1% P3OT can be regarded as P3OT being soluble in a homogeneous PMMA/EVA20 phase. Neglecting the EVA20, 1% P3OT in 90% PMMA is $\sim$ 1.11%, which is still below the critical composition of P3OT in PMMA based on the conclusion drawn from Figure 2. Thus, P3OT can be considered to be soluble in PMMA in 1/90/9 system. Similarly, after calculating the relative composition between P3OT and EVA20 in this ternary blend without considering PMMA, the relative weight ratio of P3OT/EVA20 is 10/90, which is still below the critical phase-separate composition according to Figure 1.

Since the compatibility is found in 1%P3OT/PMMA/EVA20, P3OT molecules are uniformly distributed in the PMMA/EVA20 matrix, and the continuity of conjugation might be significantly reduced because of the loss of intermolecular connectivity due to the dilute concentration of P3OT molecules in the matrix. Therefore, the miscible system is not favorable for preparing a conjugated route in the ternary blend with just 1% P3OT.

To create a continuous conjugated morphology, ternary system with higher P3OT composition (5%) are prepared and the optical pictures are shown in Figure 8. In Figure 8(a) of 5/5/90, sample color is red and no significant phase-separated phenomenon can be seen even with equal amount (5/5) of P3OT, and EVA20 are present in the ternary blend even though P3OT is easily precipitated out from matrix when PMMA is increased due to their poor interaction. As illustrated in Figure 8(b), when weight percentage of PMMA and EVA20 are equal (47.5/47.5) to each other, they separated from each other and most of the P3OT goes with the EVA20-rich phase and the mixed P3OT/EVA20 material creates a continuous red phase within the PMMA-rich matrix, which was not found in 1% P3OT ternary system. Most of the P3OT is soluble in the EVA20 phase, giving a red color of the continuous strip in the light PMMA-rich phase that owns only small amount of P3OT. The UV–vis spectra also show an additional $\lambda_{max}$ around 600 nm because of the phase separation according to Figure 4(c). It is reasonable to explain why we have an orange continuous phase, which comes from the blue shift of red (around 450 nm).

Figure 8(c) illustrates morphologies of 5% P3OT/PMMA/EVA20 system with 5/55/40 in which the fraction of PMMA is slightly over that of EVA20. A separated EVA20-rich continuous phase is conceived, resembling to the morphology of 5/47.5/47.5 except the brownish color. Still, in P3OT/EVA20 phase (brownish continuous strip), the percentages

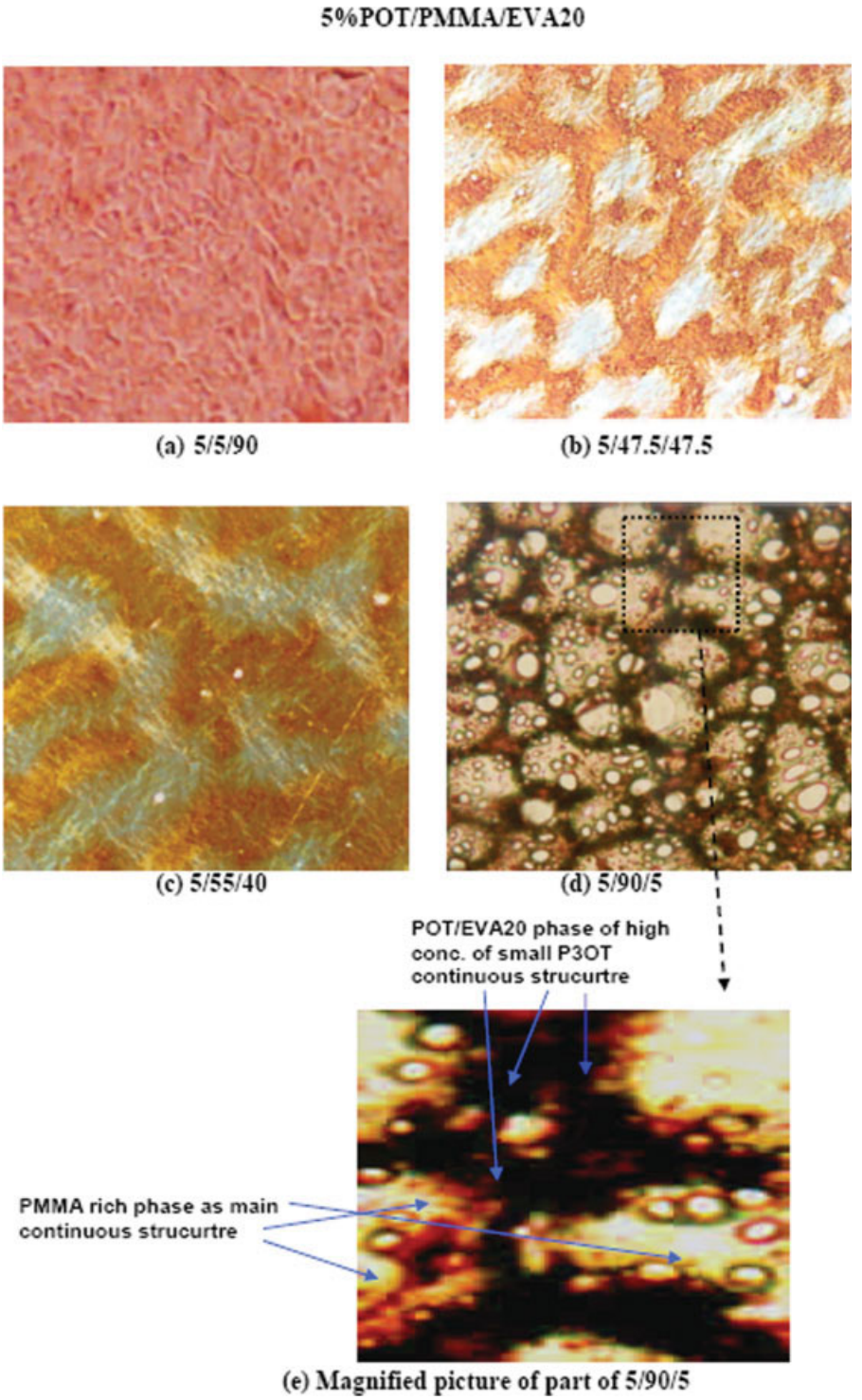


**Figure 8** Optical pictures of 5% P3OT/PMMA/EVA20 with ×100 (a) 5/5/90, (b) 5/47.5/47.5, (c) 5/55/40, (d) 5/90/5, (e) magnified picture of 5/90/5. [Color figure can be viewed in the online issue, which is available at www.interscience.wiley.com.]

of P3OT in EVA20-rich phase are about 11% (5/55) except PMMA. It does not exceed the critical composition of P3OT in EVA20 and P3OT can be uniformly spread out in the P3OT/EVA20 matrix.

When EVA20 composition is reduced to 5% and that of PMMA is increased to 90% with P3OT remains at the same composition of 5%, the P3OT/EVA20 region creates a well-defined continuous structure with clear dark red strips linked to each other in PMMA-rich matrix as shown in Figure 8(d). When we take a magnified picture of one of the strips and check the morphologies inside as shown

in Figure 8(e), we can find some dark red P3OT because of its high concentration. It seems we have morphology with one smaller continuous strips of P3OT inside P3OT/EVA20 matrix, which also forms a larger continuous structure in PMMA-rich matrix [Fig. 8(d,e)]. And it is the most favorable morphology since we have lot of P3OT molecules forming a continuous and concentrated strip to maintain a highly continuous conjugation route with the least of conjugated polymer put in the ternary polymer blend.

### Fourier transform infrared spectra

Finally, FTIR-spectra were used to identify the interactions between P3OT and PMMA or EVA20. The doublet peaks (733/721 $cm^{-1}$) of ethylene of EVA20 are because of the presence of crystallized and amorphous ethylene groups. EVA50 that is not crystallizable at room temperature has an only absorption peak in this region and there is not such absorption peaks for IR-spectrum of PVAc, which contains no ethylene groups in the backbones. A slight shift to lower wavenumbers with the increasing EVA20 in the P3OT/PMMA/EVA20 for the rocking methylenes of PMMA (752 $cm^{-1}$) can be shown in Figure 9. Even though phase separation is confirmed to be present in the 5% P3OT ternary blend with high PMMA percentages, the IR-spectra of 5% P3OT/PMMA/EVA20 as shown in Figure 10(b,c) still indicate flattened peaks of —$(CH_2)$— (752 $cm^{-1}$) rocking of PMMA. And the loss of crystallinity (disappearance of 733 $cm^{-1}$) of EVA20 in 5/5/90 system can also be seen. Therefore, the miscibility may come from either the interaction of methylene of P3OT/PMMA or P3OT/EVA20, which was also found in the conducting polymer blend based on polyaniline doped with long alkyl sulfonic acids.[35,36]

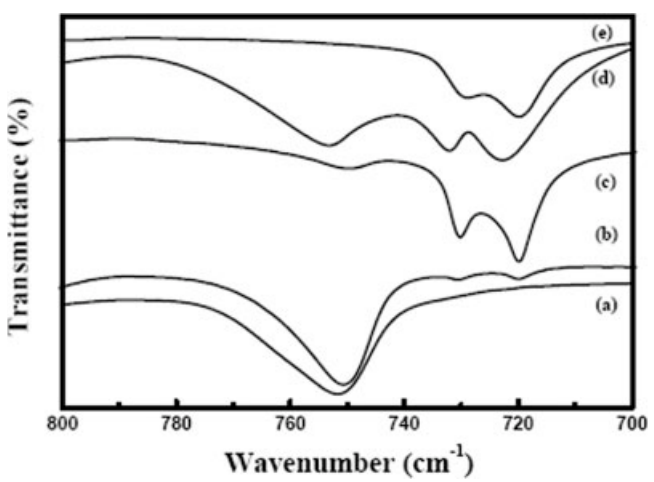


**Figure 9** FTIR spectra of 1% P3OT/PMMA/EVA20 (a) neat PMMA, (b) 1/90/9, (c) 1/49.5/49.5, (d) 1/9/90, (e) neat EVA20.

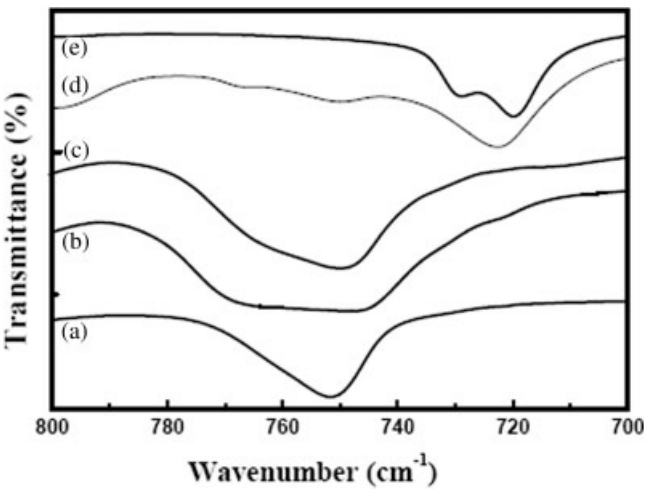


**Figure 10** FTIR spectra of 5% P3OT/PMMA/EVA20 (a) neat PMMA, (b) 5/90/5, (c) 5/47.5/47.5, (d) 5/5/90, (e) neat EVA20.

## CONCLUSIONS

The $\lambda_{max}$ of $\pi$-$\pi^*$ transition of P3OT found in the UV–vis spectrum can be used to monitor the change of the conjugation length and its miscibility with the matrix polymer in the ternary blend system. There is always a blue shift for $\lambda_{max}$ indicating that 1% P3OT is soluble in PMMA/EVA20 system. However, phase separation between EVA20 and PMMA occurs when P3OT is over 5%, resulting in the splitting of $\lambda_{max}$ with one blue shift and the other close to that of neat P3OT.

The melting point depression of EVA20 in the blend is another way to check the miscibility, which can show the good miscibility between PMMA and EVA20 in a 1% P3OT ternary blend system. In a 5% P3OT ternary system, melting point depression of EVA20 in the blend is not significant because of the extraction of EVA20 from PMMA/EVA20 matrix by 5% P3OT.

The optical microscopic pictures show uniform color when 1% P3OT is in the ternary system. Phase separation can be easily seen with 5% P3OT in P3OT/PMMA/EVA20 system. When PMMA composition is reduced, the system still illustrates a uniform morphology. High PMMA composition results in a phase separation of EVA20 from PMMA in the ternary system. Especially, morphology with one continuous dark red strips of concentrated P3OT is found to be inside P3OT/EVA20, which also forms a larger continuous structure in PMMA-rich matrix with 5/90/5 in the 5% P3OT/PMMA/EVA20 system. It is similar to the so-called fractal morphology that always demonstrates a same repeating structure after magnification. This kind of morphology is the one of the most favorable patterns for obtaining a high conjugated route inside nonconjugated matrix with the least of conjugated polymer.

From the shifting and flattening of alkyl groups of EVA20 and PMMA in FTIR spectra, we understand that the possible interaction of P3OT with EVA20 or PMMA is from the alkyl affinity between P3OT and EVA20 or PMMA, respectively.

## References


1. Flory, P. J. Macromolecules 1978, 11, 1138.
2. Prevorsek, D. C. In Polymer Liquid Crystal, 1st ed.; Cefferi, A.; Krigbaum, W. R.; Meyer, R. B., Eds.; Academic Press: New York, 1982; p 329.
3. Ho, K. S. Miscibility and Order Formation of Alkylated Rigid Polymers and Their Blends; Ph. D. Dissertation, Polymer Engineering and Science Program, Polytechnic University, 1992.
4. Levon, K.; Pashkovich, E.; Park, K. C. In Electrical and Optical Polymer Systems, Vol. 5; Wnek, G., Wise, D., Eds.; Marcel Dekker: New York, 1997; p 137.
5. Park, K. C.; Levon, K. Macromolecules 1997, 30, 3175.
6. Levon, K.; Park, K. C.; Cai, C. Synth Met 1997, 84, 335.
7. Hsu, M.; Ho, K.-S.; Kwei, T. K.; Levon, K.; Myerson, A.S. Macromolecules 1993, 26, 1318.
8. Kwei, T. K.; Levon, K.; Liu, F.; Mey-Marom, A.; Munukutla, S.; Tesoro, G. Polym Adv Technol 1993, 4, 537.
9. Kim, M. S.; Levon, K. J Polym Sci Part B: Polym Phys 1997, 7, 1025.
10. Osterholm, J.-E.; Laakso, J.; Karjalainen, S.; Mononene, P. SF Pat. 873,308 (1990).
11. Niwa, O.; Tamamura, T. Synth Met 1987, 20, 235.
12. Monederoa, M. A.; Luengoa, G. S.; Morenoa, S.; Ortegaa, F.; Rubioa, R. G.; Prolongob, M. G.; Masegosac, R. M. Polymer 1999, 40, 5833.
13. Kanemoto, K.; Shishido, M.; Sudo, T.; Akai, I.; Hashimoto, H.; Karasawa, T. Chem Phys Lett 2005, 402, 549.
14. Masegosa, R. M.; Nava, D.; Garci, S.; Prolongob, M. G.; Salom, C. Thermochim Acta 2002, 385, 85.
15. Musa, I.; Baxendale, M.; Amaratunga, G. A. J.; Eccleston, W. Synth Met 1999, 102, 1250.
16. Kymakis, E.; Alexandou, I.; Amaratunga, G. A. J. Synth Met 2002, 127, 59.
17. Camaioni, N.; Catellani, M.; Luzzati, S.; Migliori, A. Thin Solid Films 2002, 403/404, 489.
18. Erb, T.; Raleva, S.; Zhokhavets, U.; Gobsch, G.; Stuhn, B.; Spode, M.; Ambacher, O. Thin Solid Films 2004, 450, 97.
19. Stauffer, D. Phys Rep 1979, 54, 1.
20. Hotta, S.; Rughooputh, S. D. D. V.; Heeger, A. J. Synth Met 1987, 22, 79.
21. Aldissi, M.; Bishop, A. R. Polymer 1985, 26, 622.
22. Rabeony, M.; Sowa, J. M.; Berluche, E.; Ramakrishan, S.; Peiffer, D. G. Mater Res Soc 1990, EA-22, 179. Extended Abstracts.
23. Inaba, N.; Sato, K.; Suzuki, S.; Hashimoto, T. Macromolecules 1986, 19, 1690.
24. Machado, J. M.; Schlenoff, J. B.; Karasz, F. E. Macromolecules 1989, 22, 1964.
25. Laakso, J.; Osterholm, J.-E.; Nyholm, P. Synt Met 1989, 28, C467.
26. Ho, K. S.; Zheng, W. Y.; Mao, J.; Laakso, J.; Levon, K. Synth Met 1993, 55–57, 3591.
27. Levon, K.; Chu, E.; Ho, K. S.; Kwei, T. K.; Mao, J.; Zheng, W. Y.; Laakso, J. J Polym Sci Part B: Polym Phys 1995, 33, 537.
28. Yamanobe, T.; Tsukahara, M.; Komoto, T.; Watanabe, J.; Ando, I.; Uematsu, I.; Geguchi, K.; Fujito, T.; Imanari, M. Macromolecules 1988, 21, 48.
29. Sone, M.; Harkness, B. R.; Kurosu, H.; Ando, I.; Watanabe, J. Macromolecules 1994, 27, 2769.
30. Oztemiz, S.; Beaucage, A. G.; Ceylan, A. O.; Mark, H. B., Jr. J Solid State Electrochem 2004, 8, 928.
31. Pinoit, D.; Prud'homme, R. E. Polymer 2002, 43, 2321.
32. Zidan, H. M.; Tawansil, A., Abu-Elnader, M. Phys B 2003, 339, 78.
33. Lee, W. K.; Cho, W. J.; Ha, C. S.; Takahara, A.; Kajiyama, T. Polymer 1995, 36, 1229.
34. Bernini, U.; Malinconico, M.; Martuscelli, E.; Mormile, P.; Novellino, A.; Russo, P.; Volpe, M. G. J Mater Process Technol 1995, 55, 224.
35. Ho, K. S.; Hsieh, T. H.; Kuo, C. W.; Lee, S. W.; Lin, J. J.; Huang, Y. J. J Polym Sci Part A: Polym Chem 2005, 43, 3116.
36. Ho, K. S.; Hsieh, T. H.; Kuo, C. W.; Lee, S. W.; Huang, Y. J.; Chuang, C. N. J Appl Polym Sci 2006, 103, 2120.